Robotica (2005) volume 23, pp. 543–553. © 2005 Cambridge University Press
doi:10.1017/S0263574704001262 Printed in the United Kingdom

# Singularities of manipulators with non-unilateral constraints

Jingzhou Yang* and Karim Abdel-Malek

*US Army Virtual Soldier Research Program, Center for Computer-Aided Design, The University of Iowa, 111 Engineering Research Facility, Iowa City, IA 52242-1000 (USA)*

(Received in Final Form: October 31, 2004)

## SUMMARY

An analytical method is presented to obtain all surfaces enveloping the workspace of a general *n* degree-of-freedom mechanism with non-unilateral constraints. The method is applicable to kinematic chains that can be modeled using the Denavit-Hartenberg representation method for serial kinematic chains or its modification for closed-loop kinematic chains. The method developed is based upon analytical criteria for determining singular behavior of the mechanism. Singularities of manipulators with non-unilateral constraints have never been reported. The complete mathematical formulation is presented and illustrated using 4 & 5 DOF spatial manipulators. Four types of singularities are classified: Type I sets are position Jacobian singularities; Type II sets are instantaneous singularities that are due to a generalized joint are reaching its apex; Type III sets are domain boundary singularities, which are associated with the time initial and final values of the time interval; Type IV sets are coupled singularities, which are associated with a relative singular Jacobian, where the null space is reduced in one submatrix due to either of two occurrences: a Type II and Type III singularities.

KEYWORDS: Non-unilateral; Singularity; Jacobian row rank deficiency.

## I. INTRODUCTION

Numerical methods for determining boundaries of workspaces of mechanisms and manipulators have been developed by a number of authors in recent years. The importance of the study of manipulator workspaces stems from the need to better understand their functionality related to issues such as manipulator design, placement, and utilization.

Some of the earliest studies on the subject of manipulator performance in terms of workspace were conducted by Vinagradov,[1] where the term service sphere was introduced. A study of the relationship between the kinematic geometry and manipulator performance, including the workspace, was presented by Roth.[2] A numerical approach to this problem was formulated and solved by Kumar and Waldron[3] via tracing boundary surfaces of a workspace. Tsai and Soni[4] studied accessible regions of planar manipulators, while Gupta and Roth[5] studied the effect of hand size on workspace analysis. Other studies on the subject of manipulator workspaces can be found in Gupta,[6] Sugimoto and Duffy,[7] and Davidson and Hunt.[8] Other works that have dealt with manipulator workspace are reported by Yang and Lee,[9] Agrawal,[10] Gosselin and Angeles,[11] and Emiris.[12]

Pennock and Kassner[13] presented a numerical algorithm for the general study of a planar three degree-of-freedom manipulator. Cecarelli[14] used an algebraic formulation of a workspace boundary to formulate design equations of three-revolute manipulators. More recently, Zhang et al.[15] presented the graphical representation of kinematic workspaces.

Haug et al.[16] formulated numerical criteria to find the accessible output set of a general multi-degree-of-freedom system using a continuation method to trace boundary curves suitable for the study of both open- and closed-loop manipulators. The initial criteria for this computational method were presented by Haug et al.[17] and Wang and Wu.[18] The algorithm computes tangent vectors at bifurcation points of continuation curves that define the boundary of manipulator workspaces. A cross-section of the workspace is obtained and boundary continuation curves are traced. The method was demonstrated for a closed-loop mechanism called the Stewart Platform,[19] where continuation curves are evaluated on the exterior boundary of the accessible output set. These curves are then assembled into a mesh that is enveloped by appropriate surface patches. This method has proved valid for determining the general shape of the accessible output set. The main difficulty is in determining the status of a singularity at points along continuation curves. Although singular behavior occurring at points along the curves is identified, this method is completely numerical and only traces boundary curves. It does not result in analytical surfaces bounding the accessible output set. More recently, an algebraic formulation to determine the workspace of four-revolute manipulators was presented by Cecarelli and Vinciquerra.[20] The benefit of this method is shown in the ability to determine holes and voids in the accessible output set. The use of the basis of the nullspace was first introduced by Spanos and Kohli.[21]

The use of the basis of the null space criteria was first introduced by Spano and Kohli.[21] The consideration of joint limits in the study of manipulator workspaces was presented in a recent study by Delmas.[22]

Bulca et al.[23] developed a technique based on the Euler-Rodrigues parameters of the rotation of a rigid body to determine the workspace of spherical platform mechanisms. The workspace boundary is characterized by the occurrence of manipulator singularity. The singularity locus is obtained

* Author to whom all correspondence should be addressed. E-mail: jyang@engineering.uiowa.edu

both as a set of two implicit functions of the four Euler-Rodrigues parameters, which thus leads to a two-parameter manifold, and as a set of two-parameter explicit functions of joint variables that yield the four Euler-Rodrigues parameters of the rotation of the moving platform at a singular posture.

Rastegar and Deravi[24] developed a general method to determine the workspace of manipulators. Chirikjian and Ebert–Uphoff[25] applied the convolution of functions on Lie groups to determine the workspaces through partitioning a manipulator into segments, and approximating the workspace of each segment as a density function. Wang and Chirikjian[26] proposed a diffusion-based algorithm for workspace generation of hyper-redundant manipulators by solving a partial differential equation defined on the motion group.

In earlier work,[27,28] we have used singular behavior to identify the manipulator, where unilateral constraints were considered.

In this paper we apply Jacobian row rank deficiency conditions to determining the singularities of manipulators with non-unilateral constraints, where one or more joints are described as nonlinear monotonically increasing functions of time and where each joint may or may not be independent on another.

## II. FORMULATION

Define $\mathbf{q}^* \in \Re^n$ as the vector of $n$-generalized coordinates characterizing a manipulator configuration. The vector function generated by a point on the end-effector of a serial arm written as a multiplication of rotation matrices and position vectors is expressed by

$$\mathbf{\Phi}(\mathbf{q}^*(\mathbf{t})) = \begin{bmatrix} x(\mathbf{q}^*(\mathbf{t})) \\ y(\mathbf{q}^*(\mathbf{t})) \\ z(\mathbf{q}^*(\mathbf{t})) \end{bmatrix} = \sum_{i=1}^{i=n} \left[ \prod_{j=1}^{j=i-1} {}^{j-1}\mathbf{R}_j \right] {}^{i-1}\mathbf{p}_i \quad (1)$$

where $\mathbf{q}^*(\mathbf{t}) = [q_1(t_1)\ q_2(t_2)\ \ldots\ q_n(t_n)]^T$, which are non-unilateral constraints (traditionally, $\mathbf{q}^*(\mathbf{t})$ are unilateral constraints by defining $q_i^L \le q_i \le q_i^U$, where $q_i^L$ is the lower limit and $q_i^U$ is the upper limit[27,28] that at least one of $q_i(t_i)$ is the nonlinear monotonically increasing function of time $t_i$, $\mathbf{t} = [t_1\ \ldots\ t_n]^T$ is the vector of time variables for each joint, and both ${}^i\mathbf{p}_j$ and ${}^i\mathbf{R}_j$ are defined using the Denavit-Hartenberg representation method (DH)[29,30] such that

$${}^{i-1}\mathbf{R}_i = \begin{bmatrix} \cos\theta_i & -\cos\alpha_i \sin\theta_i & \sin\alpha_i \sin\theta_i \\ \sin\theta_i & \cos\alpha_i \cos\theta_i & -\sin\alpha_i \cos\theta_i \\ 0 & \sin\alpha_i & \cos\alpha_i \end{bmatrix} \quad (2)$$

and

$${}^{(i-1)}\mathbf{p}_i = [\, a_i \cos\theta_i \quad a_i \sin\theta_i \quad d_i \,]^T \quad (3)$$

where $\theta_i$ is the joint angle from $\mathbf{x}_{i-1}$ axis to the $\mathbf{x}_i$ axis, $d_i$ is the shortest distance between $\mathbf{x}_{i-1}$ and $\mathbf{x}_i$ axes, $a_i$ is the offset distance between $\mathbf{z}_i$ and $\mathbf{z}_{i-1}$ axes, and $\alpha_i$ is the offset angle from $\mathbf{z}_{i-1}$ and $\mathbf{z}_i$ axes. The generalized variable is $q_i = d_i$ if the joint is prismatic and $q_i = \theta_i$ if the joint is revolute.

The vector function $\mathbf{\Phi}(\mathbf{q}^*(\mathbf{t}))$ characterizes the set of all points inside and on the boundary of the workspace as a function of time. The aim of this work is to determine the boundary to this set and to analytically represent it.

At a specified position in space $\mathbf{x} = [\, x^0 \ \ y^0 \ \ z^0 \,]^T$, Eq. (1) can be written as a constraint function

$$\mathbf{\Omega}(\mathbf{q}^*(\mathbf{t})) = \begin{bmatrix} x(\mathbf{q}^*(\mathbf{t})) - x^0 \\ y(\mathbf{q}^*(\mathbf{t})) - y^0 \\ z(\mathbf{q}^*(\mathbf{t})) - z^0 \end{bmatrix} \quad (4)$$

and the joint functions can be written as a constraint function

$$\mathbf{\Gamma}(\mathbf{t}) = \begin{bmatrix} q_1^*(t_1) - q_1^*(t_1^0) \\ \vdots \\ q_n^*(t_n) - q_n^*(t_n^0) \end{bmatrix} \quad (5)$$

Time vector imposed in terms of inequality constraints in the form of $t_i^L \le t_i \le t_i^U$, where $i = 1, \ldots n$, are transformed into a parametric equation by introducing a new set of generalized coordinates $\boldsymbol{\lambda} = [\lambda_1, \lambda_2, \ldots, \lambda_n]^T$ such that

$$t_i = \left(\left(t_i^L + t_i^U\right)/2\right) + \left(\left(t_i^U - t_i^L\right)/2\right) \sin\lambda_i \quad i = 1, \ldots, n \quad (6)$$

These generalized coordinates $\lambda_i$ are called *slack variables* in the field of optimization.

In order to include the effect of joints with non-unilateral constraints and time limits, it is proposed to augment the constraint equation $\mathbf{\Omega}(\mathbf{q}^*)$ with the parameterized inequality constraints such that

$$\mathbf{H}(\mathbf{q}) = \begin{bmatrix} x(\mathbf{q}^*(\mathbf{t})) - x^0 \\ y(\mathbf{q}^*(\mathbf{t})) - y^0 \\ z(\mathbf{q}^*(\mathbf{t})) - z^0 \\ q_i^*(t_i) - q_i^*(t_i^0) \\ t_i - \left(\left(t_i^L + t_i^U\right)/2\right) - \left(\left(t_i^U - t_i^L\right)/2\right) \sin\lambda_i \end{bmatrix} \quad i = 1, \ldots n \quad (7)$$

where $\mathbf{q} = [\mathbf{q}^{*T}\ \ \mathbf{t}^T\ \ \boldsymbol{\lambda}^T]^T$ is the vector of all generalized coordinates. Note that although, $2n$ − new variables ($t_i$ and $\lambda_i$) have been added, $2n$ − equations have also been added to the constraint vector function without losing the dimensionality of the problem.

The *Jacobian* of the constraint function $\mathbf{H}(\mathbf{q})$ at a point $\mathbf{q}^0$ is the $(3 + 2n) \times 3n$ matrix

$$[\mathbf{H}_\mathbf{q}(\mathbf{q}_o)] = [\partial\mathbf{H}/\partial\mathbf{q}] \quad (8)$$

where the subscript denotes a derivative. With the modified formulation including the parameterized inequality constraints, the Jacobian is expanded as

$$[\mathbf{H}_\mathbf{q}] = \begin{bmatrix} \mathbf{\Phi}_{\mathbf{q}^*} & \mathbf{0}_1 & \mathbf{0}_2 \\ \mathbf{I} & \mathbf{\Gamma}_\mathbf{t} & \mathbf{0}_3 \\ \mathbf{0}_4 & \mathbf{I} & \mathbf{t}_\boldsymbol{\lambda} \end{bmatrix} \quad (9)$$

https://doi.org/10.1017/S0263574704001262 Published online by Cambridge University Press

where the notation $x_{q_1}$ denotes the partial derivative of $x$ with respect to $q_1$, and

$$[\mathbf{\Phi}_{\mathbf{q}^*}] = \begin{bmatrix} x_{q_1} & x_{q_2} & \cdots & x_{q_n} \\ y_{q_1} & y_{q_2} & \cdots & y_{q_n} \\ z_{q_1} & z_{q_2} & \cdots & z_{q_n} \end{bmatrix} \tag{10}$$

$$[\mathbf{\Gamma}_\mathbf{t}] = [\dot{\mathbf{q}}^*] = \begin{bmatrix} \dfrac{dq_1^*}{dt_1} & 0 & \ldots & 0 \\ 0 & \dfrac{dq_2^*}{dt_2} & \ldots & 0 \\ 0 & 0 & \ldots & 0 \\ 0 & 0 & \ldots & \dfrac{dq_n^*}{dt_n} \end{bmatrix} \tag{11}$$

and

$$[\mathbf{t}_\lambda] = \begin{bmatrix} -\left((t_1^U - t_1^L)/2\right)\cos\lambda_1 & 0 & \ldots & 0 \\ 0 & -\left((t_2^U - t_2^L)/2\right)\cos\lambda_2 & \ldots & 0 \\ 0 & 0 & \ldots & 0 \\ 0 & 0 & \ldots & -\left((t_n^U - t_n^L)/2\right)\cos\lambda_n \end{bmatrix} \tag{12}$$

is a diagonal block matrix, $\mathbf{0}_2$ and $\mathbf{0}_1$ are $(3 \times n)$ zero matrices, $\mathbf{0}_3$ and $\mathbf{0}_4$ are $(n \times n)$ zero matrices and $\mathbf{I}$ is $(n \times n)$ identity matrix.

The *boundary to the workspace* $\partial W$ (workspace envelope) is a subset of the *workspace* at which the Jacobian of the constraint function of Eqs. (8) and (9) is row rank deficient, i.e.,

$$\partial W \subset \{\text{Rank } \mathbf{H}_\mathbf{q}(\mathbf{q}) < k, \text{for some } \mathbf{q} \text{ with } \mathbf{H}(\mathbf{q}) = \mathbf{0}\} \tag{13}$$

where $k$ is at least $(3 + 2n - 1)$. For an $n$-DOF system, the Jacobian $\mathbf{H}_\mathbf{q}(\mathbf{q}^o)$ is row-rank deficient if and only if one of the following conditions are satisfied.

*I.1. Type I singularities*

If no $t_i$ have reached their limits, which says $t_i \neq t_i^U$ and $t_i \neq t_i^L$, and no joints with $\frac{dq_i}{dt_i} \neq 0$, the diagonal sub-matrices $[\mathbf{\Gamma}_\mathbf{t}]$ and $[\mathbf{t}_\lambda]$ are full row rank. Therefore, the only possibility for $[\mathbf{H}_\mathbf{q}]$ to be row-rank deficient is when the block matrix $[\mathbf{\Phi}_{\mathbf{q}^*}]$ is row rank deficient. Define two independent sub-vectors of $\mathbf{q}^*$ as $\mathbf{p}$ and $\mathbf{u}$, as

$$\mathbf{q}^* = [\mathbf{p}^T \ \ \mathbf{u}^T]^T, \text{where } \mathbf{p}, \mathbf{u} \in \mathbf{q}^* \text{and } \mathbf{p} \cap \mathbf{u} = \phi \tag{14}$$

If $\mathbf{u} \in \mathbf{R}^m$ then $\mathbf{p} \in \mathbf{R}^{(n-m)}$.

**Type I singularity set** can be defined as

$$S^{(1)} \equiv \{\mathbf{p} \in \mathbf{q}^* : \text{Rank}[\mathbf{\Phi}_{\mathbf{q}^*}] < 3, \text{ for some constant subset of } \mathbf{q}\} \tag{15}$$

where $\mathbf{p}$ is within the specified joint limit constraints.

The $(m \times n)$ block matrix $[\mathbf{\Phi}_{\mathbf{q}^*}]$ is row rank deficient at least one, where $m = 3$ for spatial and $m = 2$ for planar manipulators. The rank of the $(m \times n)$ matrix is defined to be the order of the largest non-singular square sub-matrix which can be formed by selecting rows and columns of the upper corner matrix $[\mathbf{\Phi}_{\mathbf{q}^*}]$. In order to make the sub-matrix $[\mathbf{\Phi}_{\mathbf{q}^*}]$ rank deficient of order $(d)$ where $d = \text{abs}(m - n)$, it is necessary to determine all sub-Jacobians. For a rank-deficiency $(d)$, the largest square sub matrix cannot have a larger dimension than $b = \max(n - d, m - d)$. Therefore, there must be $m!/[(m-b)!b!]$ possible independent rows that can be considered in a single square sub-matrix. Similarly, there are $n!/[(n-b)!b!]$ possible combinations of columns. Hence, there exists

$$\eta = \frac{n!}{(n-b)!b!} \cdot \frac{m!}{(m-b)!b!} \tag{16}$$

sub-Jacobians. Equating the determinants to zero yields $\eta$-number of equations to be solved simultaneously. The solutions to these $\eta$ equations are the **singular sets of Type I**. This criterion is used to obtain square sub-Jacobians. Solutions of the resulting $\eta$ equations are sets of constant generalized coordinates denoted by $\mathbf{p}_i$ and are characterized by the following set

$$\mathbf{p}_i = \left\{ \begin{bmatrix} \det(\hbar_i \hbar_j \hbar_k)_1 \\ \vdots \\ \det(\hbar_i \hbar_j \hbar_k)_\eta \end{bmatrix} = \mathbf{0}, \right. \\ \left. \text{for } i, j, k = 1, \ldots, n \text{ and } i \neq j \neq k \right\} \quad i = 1, 2, \ldots, \beta \tag{17}$$

where $\hbar_i$ denotes a column of the matrix $[\mathbf{\Phi}_{\mathbf{q}^*}] = [\hbar_k, \ldots, \hbar_m]$. For each $\mathbf{p}_i$, the remaining variables are $\mathbf{u}_i$.

*I.2. Type II (Instantaneous) singularities*

When we find there are $m(m \geq 2)$ joints that have $\frac{dq_i^*}{dt_i} = 0$, then Type III singularities are

$$S^{(2)} \equiv \left\{\mathbf{p} \in \Re^{(n-2)} : \mathbf{p} \equiv \partial \mathbf{t}^{\text{inst}} = \left[t_i^{\text{inst}}, t_j^{\text{inst}}, \ldots\right]\right\} \tag{18}$$

This type of singularities comes from the non-unilateral constraints.

*I.3. Type III singularities*

Type III singularities are defined as

$$S^{(3)} \equiv \left\{\mathbf{p} \in \Re^{(n-2)} : \mathbf{p} \equiv \partial \mathbf{t}^{\text{inst}} \cup \partial \mathbf{t}^{\text{Limit}} \right. \\ \left. = \left[t_i^{\text{inst}}, t_j^{\text{inst}}, \ldots\right] \cup \left[t_i^{\text{limit}}, t_j^{\text{limit}}, \ldots\right]\right\} \tag{19}$$

*I.4. Type IV singularities (Coupled Singularities)*

When certain $t_i$ reach their limits, e.g., $[t_i, t_j, t_k] = [t_i^{\text{limit}}, t_j^{\text{limit}}, t_k^{\text{limit}}]$, the corresponding diagonal elements in the matrix $[\mathbf{t}_\lambda]$ will be equal to zero. For example, if $t_i = t_i^L$, the diagonal element of $[\partial \mathbf{t}/\partial \boldsymbol{\lambda}]_{ii}$ will be zero (i.e., $b_i \cos\lambda_i$ is zero for either $i = 1, \ldots, n$ then $t_i$ has reached a limit). When certain $t_i$ reach their instantaneous points (say $\frac{dq_i^*}{dt_i} = 0$), e.g., $[t_i, t_j, t_k] = [t_i^{\text{inst}}, t_j^{\text{inst}}, t_k^{\text{inst}}]$, the corresponding diagonal elements in the matrix $[\mathbf{\Gamma}_\mathbf{t}]$ will be equal to zero.

https://doi.org/10.1017/S0263574704001262 Published online by Cambridge University Press

Solving the row rank deficiency condition for Eq. (9) is equivalent to solving the rank deficiency for

$$\left[\mathbf{\Phi}_{\mathbf{q}^*} \not\subset \left[\mathbf{\Phi}_{q_i}, \mathbf{\Phi}_{q_j}, \mathbf{\Phi}_{q_k}\right]\right], \tag{20}$$

with

$$q_i = q_i^{\text{limit}}, q_j = q_j^{\text{limit}}, q_k = q_k^{\text{limit}}$$
$$or\, q_i = q_i^{\text{inst}}, q_j = q_j^{\text{inst}}, q_k = q_k^{\text{inst}}$$

where the notation of represents the exclusion of the right matrix from the left matrix and it represents the sub-matrix of $[\mathbf{\Phi}_{\mathbf{q}^*}]$ when $t_i$ are at their limits or instantaneous points.

From the foregoing observation, the second type of singular sets is formulated. Define a new vector $\partial\mathbf{q}(\mathbf{t}^{\text{limit}}) = [q_i(t^{\text{limit}}), q_j(t^{\text{limit}}), q_k(t^{\text{limit}})]^T$, or $\partial\mathbf{q}(\mathbf{t}^{\text{inst}}) = [q_i(t^{\text{inst}}), q_j(t^{\text{inst}}), q_k(t^{\text{inst}})]^T$, which is a sub-vector of $\mathbf{q}^*$ where

$$1 \le \dim(\partial\mathbf{q}(\mathbf{t}^{\text{limit}}\ or\ \mathbf{t}^{\text{inst}})) \le (n-3) \tag{21}$$

For the case of $\dim(\partial\mathbf{q}(\mathbf{t}^{\text{limit}}\ or\ \mathbf{t}^{\text{inst}}) = (n-2)$ it is noted that the solution of Eq. is readily available as will be discussed in the following paragraphs. The joint coordinates can be partitioned as

$$\mathbf{q}^* = [\mathbf{w}^T, \partial\mathbf{q}(\mathbf{t}^{\text{limit}}\ or\ \mathbf{t}^{\text{inst}})^T]^T, \text{ and } \mathbf{w} \cap \partial\mathbf{q}(\mathbf{t}^{\text{limit}}\ or\ \mathbf{t}^{\text{inst}}) = \phi \tag{22}$$

Then, if $[\mathbf{\Phi}_{\mathbf{w}}(\mathbf{w}, \partial\mathbf{q}(\mathbf{t}^{\text{limit}}\ or\ \mathbf{t}^{\text{inst}}))]$ is row rank deficient, the sub-Jacobian $[\mathbf{\Phi}_{\mathbf{q}^*}]$ is also rank deficient. Let the solution for this condition be denoted by $\hat{\mathbf{p}}$, which is a constant sub-vector of $\mathbf{w}$, and $\mathbf{w} = [\mathbf{u}^T, \hat{\mathbf{p}}^T]^T$. The **type IV singularity** set is defined as

$$\begin{aligned} S^{(4)} \equiv \big\{ & \mathbf{p} = [\hat{\mathbf{p}} \cup \partial\mathbf{q}(\mathbf{t}^{\text{limit}}\ or\ \mathbf{t}^{\text{inst}})] : \\ & \text{Rank}[\mathbf{\Phi}_{\mathbf{q}^*}(\mathbf{w}, \partial\mathbf{q}(\mathbf{t}^{\text{limit}}\ or\ \mathbf{t}^{\text{inst}}))] < 3, \\ & for\ some\ \hat{\mathbf{p}} \in \mathbf{w}, \mathbf{dim}(\partial\mathbf{q}(\mathbf{t}^{\text{limit}}\ or\ \mathbf{t}^{\text{inst}})) \le (n-3) \big\} \end{aligned} \tag{23}$$

## II. ILLUSTRATIVE EXAMPLES

In this section we will use two examples to demonstrate the formulation to determine the singular surfaces of the manipulators with non-unilateral constraints. The first one is a 4DOF spatial example and the second one is a 5DOF spatial example.

### *II.1. 4DOF RPRP example*

A spatial 4-DOF manipulator as shown in Fig. 1 will be used to demonstrate the proposed method determining the singularities and the DH table is shown in Table 1.

The manipulator has two revolute and two prismatic joints. The joint profiles are defined by the following equations and shown in Fig. 2.

$$q_1(t_1) = \pi t_1 \tag{24}$$

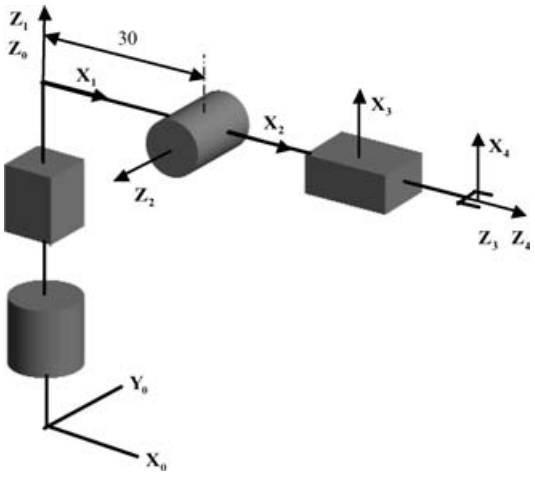


Fig. 1. The spatial 4-DOF RPRP manipulator.

Table I. DH table for a spatial 4-DOF manipulator.

| | $\theta_i$ | $d_i$ | $\alpha_i$ | $a_i$ |
|---|---|---|---|---|
| 1 | $q_1$ | 0 | 0 | 0 |
| 2 | 0 | $q_2$ | $\pi/2$ | 30 |
| 3 | $\pi/2 + q_3$ | 0 | $\pi/2$ | 0 |
| 4 | 0 | $q_4$ | 0 | 0 |

$$q_2(t_2) = 12t_2 + 20 \tag{25}$$

$$q_3(t_3) = -\frac{7\pi}{4}t_3^2 + 3.5\pi t_3 - \frac{\pi}{4} \tag{26}$$

$$q_4(t_4) = -6.667t_4^2 + 20t_4 + 10 \tag{27}$$

where $0 \le t_1 \le 2$, $0 \le t_2 \le 2.5$, $0 \le t_3 \le 1.53452$, $0 \le t_4 \le 2.36586$.

For the joint frames selected in Fig. 2, the position vector of the end-effector is formulated as

$$\mathbf{x} = \mathbf{\Phi}(\mathbf{q}(\mathbf{t})) = \begin{bmatrix} q_4 \cos q_1 \cos q_3 + 30 \cos q_1 \\ q_4 \sin q_1 \cos q_3 + 30 \sin q_1 \\ q_4 \sin q_3 + q_2 \end{bmatrix} \tag{28}$$

and the inequality constraints are parameterized as $t_1 = 1 + \sin\lambda_1$, $t_2 = 1.25 + 1.25\sin\lambda_2$, $t_3 = 0.76726 + 0.76726\sin\lambda_3$, and $t_4 = 1.18293 + 1.18293\sin\lambda_4$, where $\lambda = [\lambda_1\ \lambda_2\ \lambda_3\ \lambda_4]^T$.

The Jacobian matrix is derived as

$$[\mathbf{H}_{\mathbf{q}}] = \begin{bmatrix} \mathbf{\Phi}_{\mathbf{q}^*} & \mathbf{0}_1 & \mathbf{0}_2 \\ \mathbf{I} & \mathbf{\Gamma}_{\mathbf{t}} & \mathbf{0}_3 \\ \mathbf{0}_4 & \mathbf{I} & \mathbf{t}_{\boldsymbol{\lambda}} \end{bmatrix}_{11\times 12} \tag{29}$$

where

$$[\mathbf{\Phi}_{\mathbf{q}^*}](\mathbf{q}) = \begin{bmatrix} -q_4 \sin q_1 \cos q_3 - 30 \sin q_1 & 0 & -q_4 \cos q_1 \sin q_3 & \cos q_1 \cos q_3 \\ q_4 \cos q_1 \cos q_3 + 30 \cos q_1 & 0 & -q_4 \sin q_1 \sin q_3 & \sin q_1 \cos q_3 \\ 0 & 1 & q_4 \cos q_3 & \sin q_3 \end{bmatrix}_{3\times 4} \tag{30}$$

https://doi.org/10.1017/S0263574704001262 Published online by Cambridge University Press

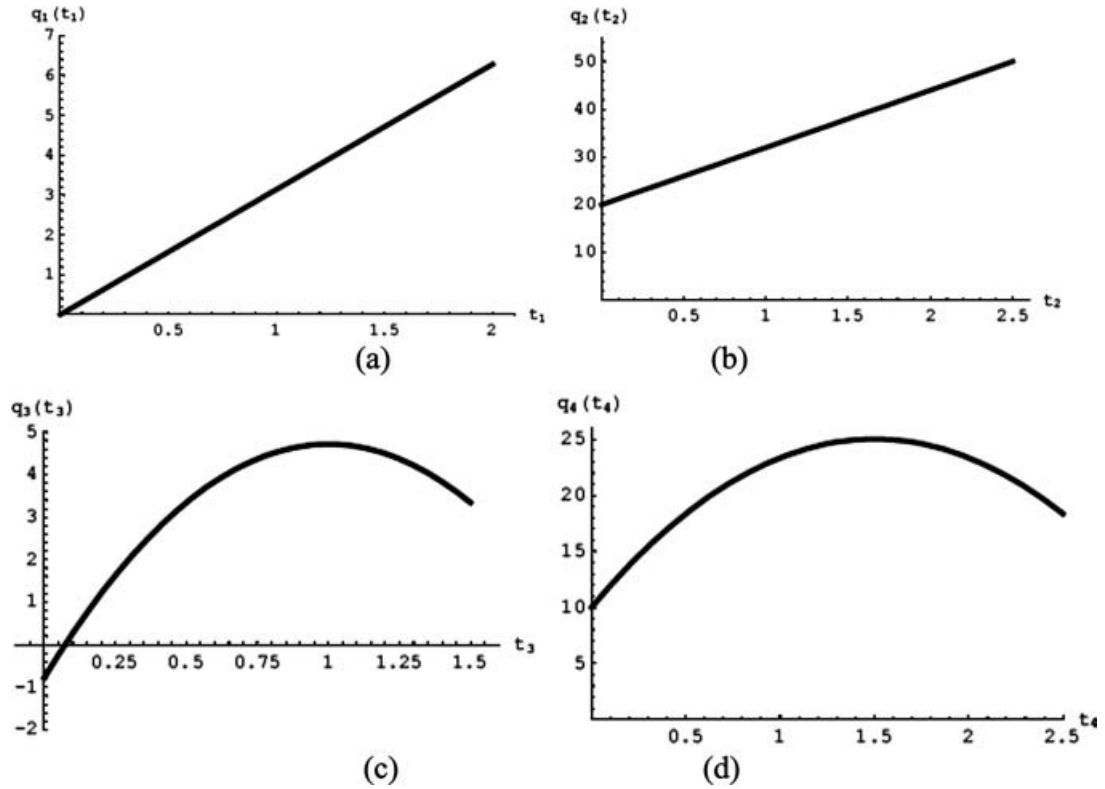


Fig. 2. Joint profiles (a) $q_1$ profile (b) $q_2$ profile (c) $q_3$ profile (d) $q_4$ profile.

$$\mathbf{\Gamma_t} = \begin{bmatrix} -\pi & 0 & 0 & 0 \\ 0 & -12 & 0 & 0 \\ 0 & 0 & 3.5\pi(t_3 - 1) & 0 \\ 0 & 0 & 0 & 13.334t_4 - 20 \end{bmatrix}_{4\times 4} \tag{31}$$

$$\mathbf{t_\lambda} = \begin{bmatrix} -\cos\lambda_1 & 0 & 0 & 0 \\ 0 & -1.25\cos\lambda_2 & 0 & 0 \\ 0 & 0 & -0.76726\cos\lambda_3 & 0 \\ 0 & 0 & 0 & -1.18293\cos\lambda_4 \end{bmatrix}_{4\times 4} \tag{32}$$

**II.1.1. Type I singularities:** Since $[\mathbf{\Phi_{q^*}}]$ is a $(3 \times 4)$ block matrix, $n = 4, m = 3$ and the deficiency criteria mandates that $d = (4 - 3)$ and $b = \max(3, 2)$. Substituting into Eq. (16) yields $\eta = 4$ equations to be solved simultaneously to be zero which represent the determinants of the $(3 \times 3)$ sub-Jacobians as

$$\begin{aligned} Det[J1] &= -q_4(30 + q4\cos q_3)\sin q_3 \\ Det[J2] &= \cos q_3(30 + q_4\cos q_3) \\ Det[J3] &= 0 \\ Det[J2] &= q_4(30 + q_4\cos q_3) \end{aligned}$$

Solution to the ten is given by $q_4 = -30\sec q_3$, this solution does not satisfy the joint profiles. Therefore the rank-deficiency criterion of the Jacobian yields no singular set.

**II.1.2. Type II (instantaneous) singularities:** From the joint profile equations $q_1(t_1)$ and $q_2(t_2)$ do not have instantaneous points. However, $\frac{dq_3(t_3)}{dt_3} = 0$ yields $t_3 = 1.0$, and $\frac{dq_4(t_4)}{dt_4} = 0$ yields $t_4 = 1.5$. Therefore singularity set is $\mathbf{p_1} = \{q_3(1.0), q_4(1.5)\}$.

**II.1.3. Type III singularities:** This includes joint outer limits and instantaneous limits combinations as follows:

$\mathbf{p}_2 = \{q_3(1.53452), q_4(0)\}$, $\mathbf{p}_3 = \{q_3(1.53452), q_4(2.36586)\}$,
$\mathbf{p}_4 = \{q_2(0), q_3(0)\}$, $\mathbf{p}_5 = \{q_2(0), q_3(1.53452)\}$,
$\mathbf{p}_6 = \{q_2(0), q_4(0)\}$, $\mathbf{p}_7 = \{q_2(0), q_4(2.36586)\}$,
$\mathbf{p}_8 = \{q_2(2.5), q_3(0)\}$, $\mathbf{p}_9 = \{q_3(2.5), q_4(0)\}$,
$\mathbf{p}_{10} = \{q_2(2.5), q_4(2.36586)\}$, $\mathbf{p}_{11} = \{q_3(0), q_4(0)\}$,
$\mathbf{p}_{12} = \{q_3(0), q_4(2.36586)\}$, $\mathbf{p}_{13} = \{q_3(1), q_4(0)\}$,
$\mathbf{p}_{14} = \{q_3(1), q_4(2.36586)\}$, $\mathbf{p}_{15} = \{q_2(0), q_3(1)\}$,
$\mathbf{p}_{16} = \{q_2(2.5), q_3(1)\}$, $\mathbf{p}_{17} = \{q_1(0), q_3(1)\}$,
$\mathbf{p}_{18} = \{q_1(2), q_3(1)\}$, $\mathbf{p}_{19} = \{q_3(0), q_4(1.5)\}$,
$\mathbf{p}_{20} = \{q_3(1.53452), q_4(1.5)\}$, $\mathbf{p}_{21} = \{q_2(0), q_4(1.5)\}$,
$\mathbf{p}_{22} = \{q_2(2.5), q_4(1.5)\}$, $\mathbf{p}_{23} = \{q_1(0), q_4(1.5)\}$,
$\mathbf{p}_{24} = \{q_1(2.5), q_4(1.5)\}$.

**II.1.4. Type IV (coupled) singularities:** The block $\mathbf{t_\lambda}$ is rank deficient at $t_4 = 0$. Substituting $t_4 = 0$ into $\mathbf{\Phi}(\mathbf{q}^*)$, computing $[\mathbf{\Phi_{q^*}}]$, then $[\mathbf{\Phi_{q^*}} \not\subset \mathbf{\Phi}_{q_4}]$ is defined as

$$\left[\mathbf{\Phi_{q^*}} \not\subset \mathbf{\Phi}_{q_4}\right] = \begin{bmatrix} -30\sin q_1 - 10\cos q_3 \sin q_1 & 0 & -10\cos q_1 \sin q_3 \\ -30\cos q_1 + 10\cos q_3 \cos q_1 & 0 & -10\sin q_1 \sin q_3 \\ 0 & 1 & 10\cos q_3 \end{bmatrix}$$

https://doi.org/10.1017/S0263574704001262 Published online by Cambridge University Press

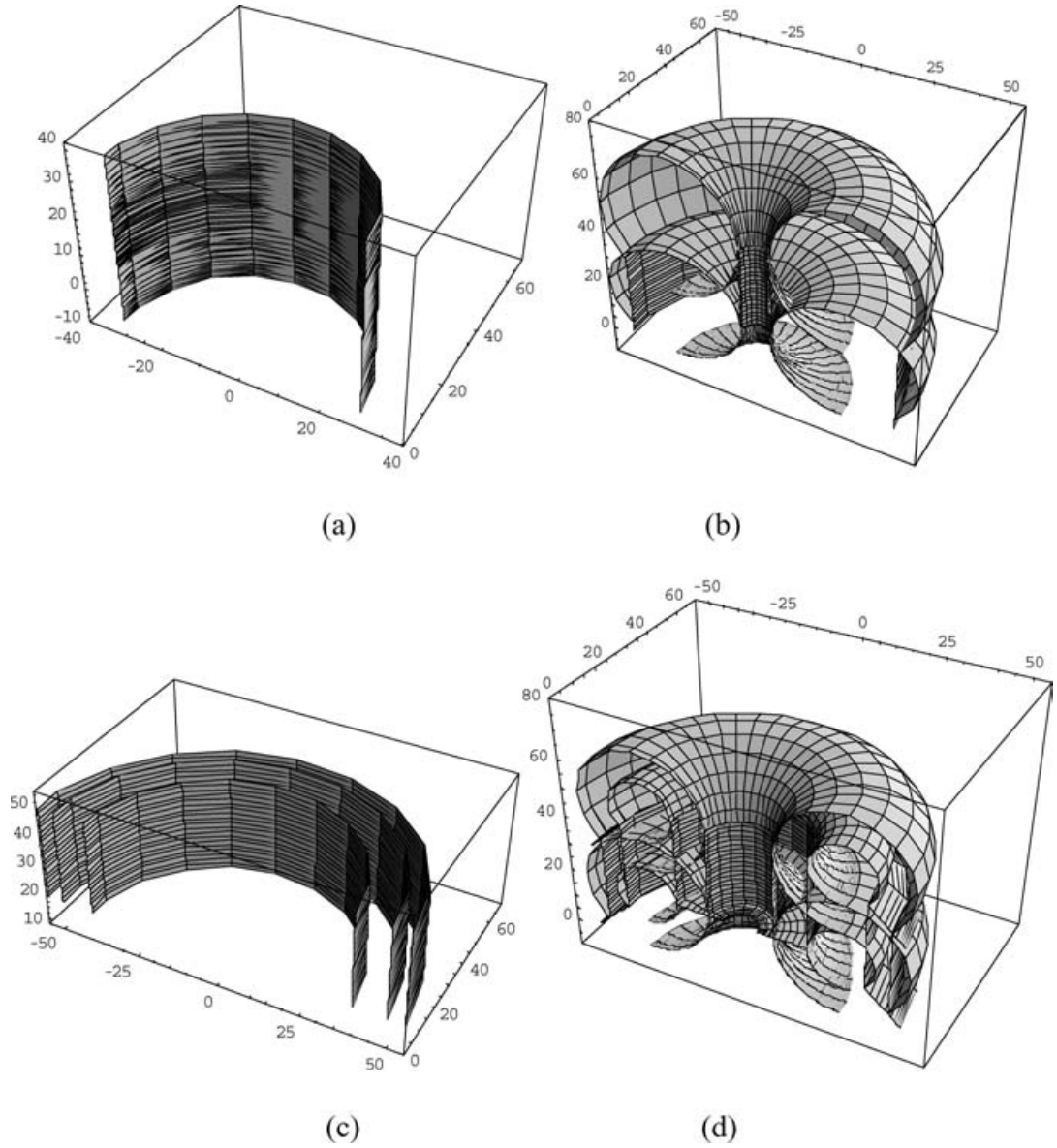


Fig. 3. Cross sections of the singular surfaces (a) Due to $\psi_1$ and $\psi_{13}, \ldots, \psi_{18}$ (b) Due to $\psi_{19}, \ldots, \psi_{21}$ (c) Due to $\psi_{25}, \psi_{26}, \psi_{27}$ (d) Due to $\psi_2, \ldots, \psi_{12}$.

and applying the rank deficiency condition to $[\mathbf{\Phi}_{\mathbf{q}^*} \not\subset \mathbf{\Phi}_{q_4}]$ where $\partial\mathbf{q}(\mathbf{t}^{\text{limit}}) = q_4(t_4^L)$ yields a solution $q_3 = 0$, which is at $t_3 = 0.07418$. Therefore a singular set identified as $\mathbf{p} = [\hat{\mathbf{p}}, \partial\mathbf{q}(\mathbf{t}^{\text{limit}})] = \mathbf{p}_{25} = \{q_3(0.07418), q_4(0)\}$, similarly, $\mathbf{p}_{26} = \{q_3(0.07418), q_4(2.36586)\}$.

The block $[\mathbf{\Gamma}_\mathbf{t}]$ is rank deficient at $t_4 = 1.5$. Substituting $t_4 = 1.5$ into $\mathbf{\Phi}(\mathbf{q}^*)$, computing $[\mathbf{\Phi}_{\mathbf{q}^*}]$, then $[\mathbf{\Phi}_{\mathbf{q}^*} \not\subset \mathbf{\Phi}_{q_4}]$ is defined

$$JJ = \begin{bmatrix} -30\sin q_1 - 25\cos q_3 \sin q_1 & 0 & -25\cos q_1 \sin q_3 \\ -30\cos q_1 + 25\cos q_3 \cos q_1 & 0 & -25\sin q_1 \sin q_3 \\ 0 & 1 & 25\cos q_3 \end{bmatrix},$$

and applying the rank deficiency condition to $JJ$ where $\partial\mathbf{q}(\mathbf{t}^{\text{inst}}) = q_4(t_4^{\text{inst}})$ yields a solution $q_3 = 0$, which is at $t_3 = 0.07418$. Therefore a singular set identified as $\mathbf{p}_{27} = \{q_3(0.07418), q_4(1.5)\}$.

Substituting each singularity set into Eq. (28) yields parametric equations of singular surfaces in $\mathbf{R}^3$. Fig. 3 shows the cross sections of singular surfaces due to different singular sets and Fig. 4 is a cross-section of the workspace volume depicting all singular surfaces.

*II.2. 5DOF RRPRR example*

Consider the 5-DOF manipulator shown in Fig. 5. It includes 4 revolute joints and 1 prismatic joint.

Joints are defined by the following profiles:

$$q_1(t_1) = \pi t_1 \tag{33}$$

$$q_2(t_2) = 1.88496t_2 - 0.785398 \tag{34}$$

$$q_3(t_3) = -2t_3^2 + 8t_3 \tag{35}$$

$$q_4(t_4) = -2.0944t_4^2 + 2\pi t_4 \tag{36}$$

$$q_5(t_5) = -\frac{3\pi}{2}t_4^2 + 3\pi t_4 - \frac{\pi}{2} \tag{37}$$

https://doi.org/10.1017/S0263574704001262 Published online by Cambridge University Press

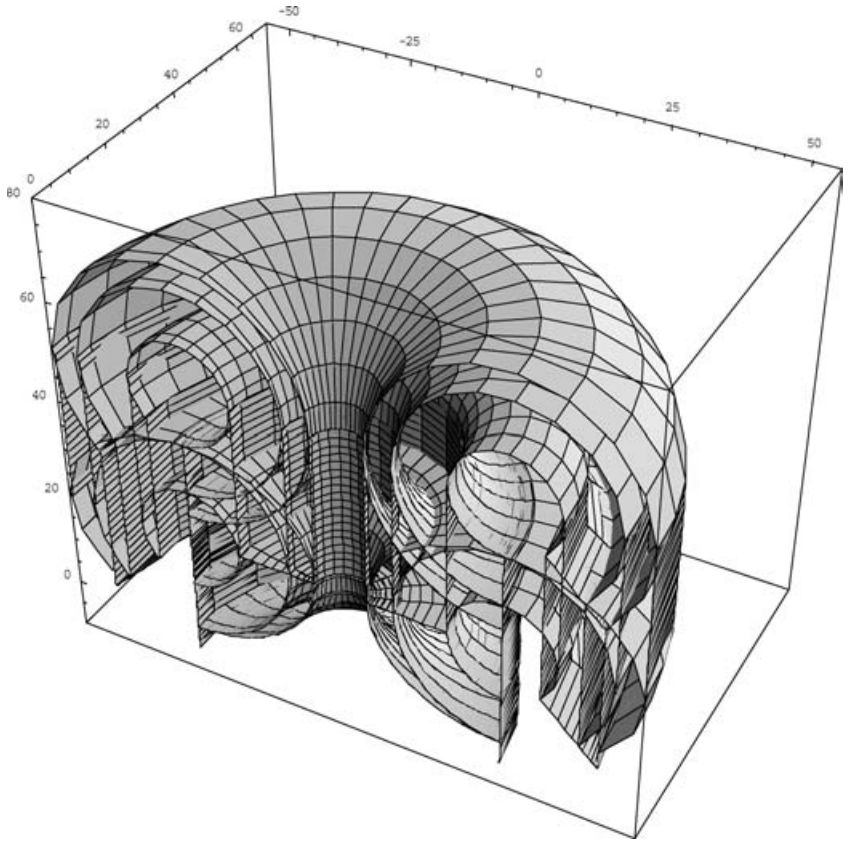


Fig. 4. Cross sections of the final workspace.

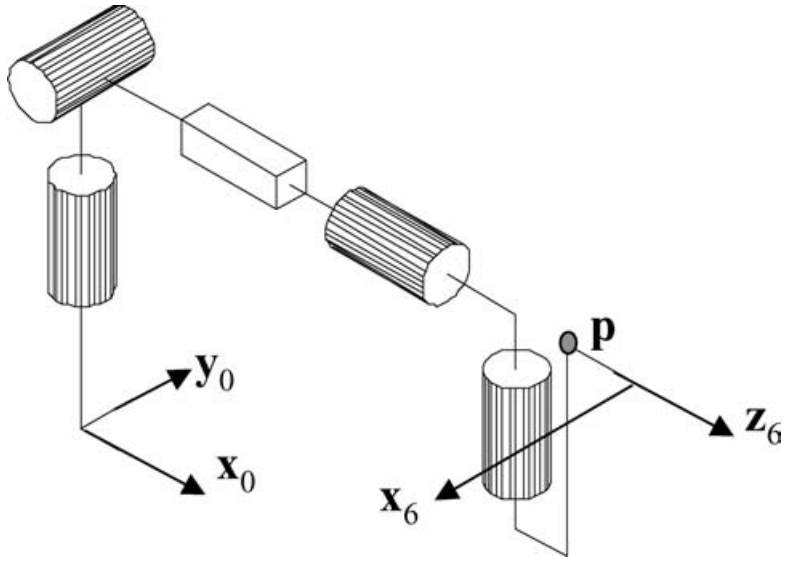


Fig. 5. The 5-DOF RRPRR Manipulator.

where $0 \le t_1 \le 2$, $0 \le t_2 \le 2.06695$, $0 \le t_3 \le 3.22474$, $0 \le t_4 \le 2.5$, $0 \le t_5 \le 1.57735$. The profiles can be plotted in Figure 6.

Using Denavit-Hartenberg, the position vector of point **p** in Fig. 7 is determined as

and the inequality constraints are parameterized as $t_1 = 1 + \sin\lambda_1$, $t_2 = 1.25 + 1.25\sin\lambda_2$, $t_3 = 1.61237 + 1.61237\sin\lambda_3$, $t_4 = 1.18301 + 1.18301\sin\lambda_4$, and $t_5 = 0.788675 + 0.788675\sin\lambda_4$, where $\lambda = [\lambda_1\ \lambda_2\ \lambda_3\ \lambda_4\ \lambda_5]^T$.

$$\mathbf{\Phi}(\mathbf{q}^*) = \begin{bmatrix} -5\sin q_5\cos q_1\sin q_2\sin q_4 - 5\sin q_5\sin q_1\cos q_4 + 5\cos q_1\cos q_2\cos q_5 + 15\cos q_1\cos q_2 + q_3\cos q_1\cos q_2 \\ -5\sin q_5\sin q_1\sin q_2\sin q_4 + 5\sin q_5\cos q_1\cos q_4 + 5\sin q_1\cos q_2\cos q_5 + 15\sin q_1\cos q_2 + q_3\sin q_1\cos q_2 \\ 5\cos q_2\sin q_4\sin q_5 + 5\sin q_2\cos q_5 + 15\sin q_2 + q_3\sin q_2 + 25 \end{bmatrix} \tag{38}$$

https://doi.org/10.1017/S0263574704001262 Published online by Cambridge University Press

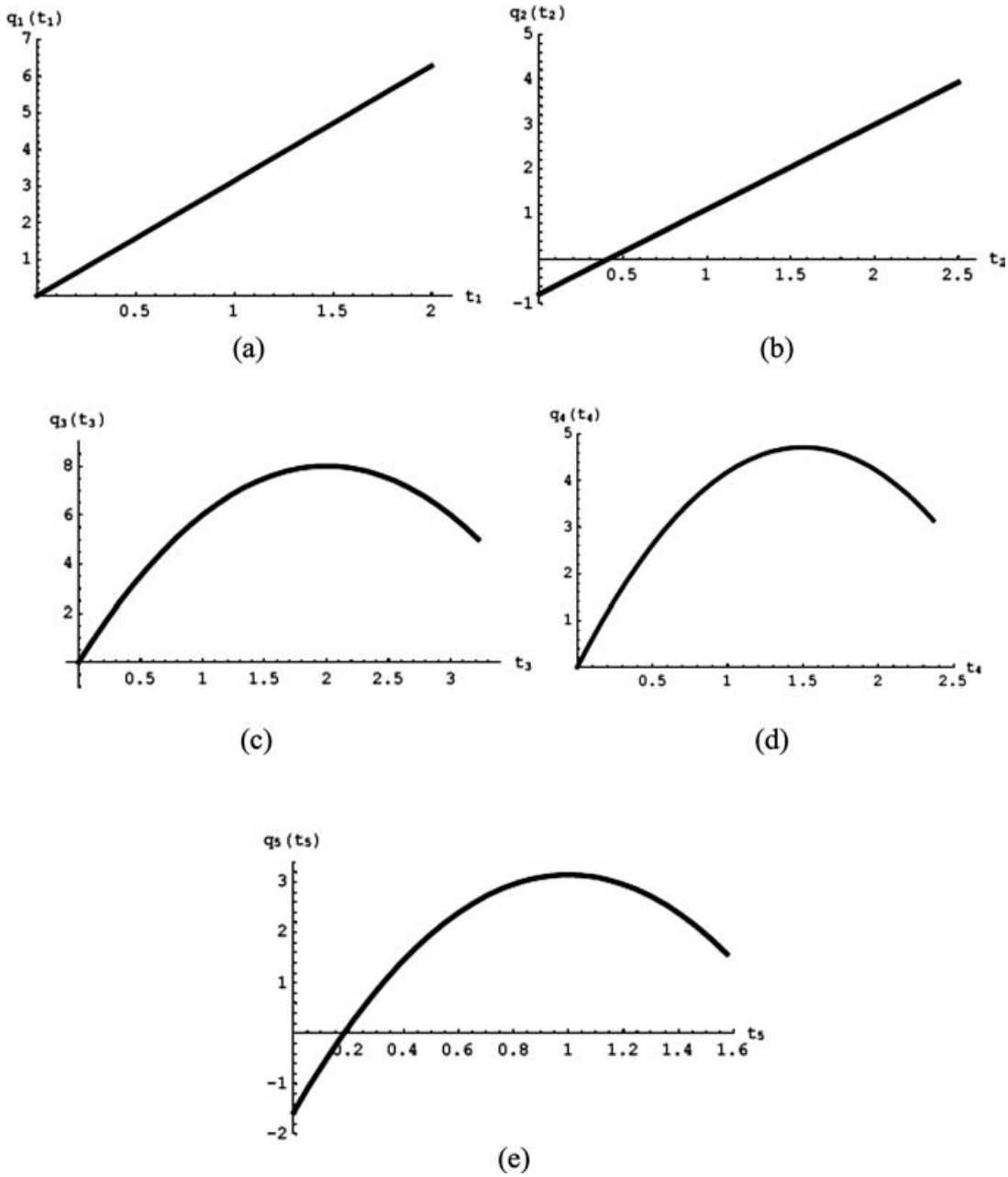


Fig. 6. The joint profiles (a) $q_1$ profile (b) $q_2$ profile (c) $q_3$ profile (d) $q_4$ profile (e) $q_5$ profile.

The Jacobian matrix is derived as

$$[\mathbf{H_q}] = \begin{bmatrix} \mathbf{\Phi_{q^*}} & \mathbf{0}_1 & \mathbf{0}_2 \\ \mathbf{I} & \mathbf{\Gamma_t} & \mathbf{0}_3 \\ \mathbf{0}_4 & \mathbf{I} & \mathbf{t_\lambda} \end{bmatrix}_{13\times 15} \tag{39}$$

where

$$[\mathbf{\Phi}_{\mathbf{q}^*}](\mathbf{q}) = \begin{bmatrix} -c_2(23+5c_5)s_1 + 5(-c_1c_4 + s_1s_2s_4)s_5 & -c_1((23+5c_5)s_2 + 5c_2s_4s_5) & 0 & 5(-c_1c_4s_2 + s_1s_4)s_5 & -5(c_4c_5s_1 + c_1(c_5s_2s_4 + c_2s_5)) \\ -5c_4s_1s_5 + c_1(c_2(23+5c_5) - 5s_2s_4s_5) & -s_1((23+5c_5)s_2 + 5c_2s_4s_5) & 0 & -5(c_4s_1s_2 + c_1s_4)s_5 & 5c_1c_4c_5 - 5s_1(c_5s_2s_4 + c_2s_5) \\ 0 & c_2(23+5c_5) - 5s_2s_4s_5 & 0 & 5c_2c_4s_5 & 5c_2c_5s_4 - 5s_2s_5 \end{bmatrix}_{3\times 5} \tag{40}$$

$$[\mathbf{\Gamma_t}] = \begin{bmatrix} -\pi & 0 & 0 & 0 & 0 \\ 0 & -1.88496 & 0 & 0 & 0 \\ 0 & 0 & 4t_3 - 8 & 0 & 0 \\ 0 & 0 & 0 & 4.1888t_4 - 6.28319 & 0 \\ 0 & 0 & 0 & 0 & 3\pi(t_5 - 1) \end{bmatrix}_{5\times 5} \tag{41}$$

$$[\mathbf{t_\lambda}] = \begin{bmatrix} -\cos\lambda_1 & 0 & 0 & 0 & 0 \\ 0 & -1.25\cos\lambda_2 & 0 & 0 & 0 \\ 0 & 0 & -1.61237\cos\lambda_3 & 0 & 0 \\ 0 & 0 & 0 & -1.18301\cos\lambda_4 & 0 \\ 0 & 0 & 0 & 0 & -0.788675\cos\lambda_5 \end{bmatrix}_{5\times 5} \tag{42}$$

https://doi.org/10.1017/S0263574704001262 Published online by Cambridge University Press

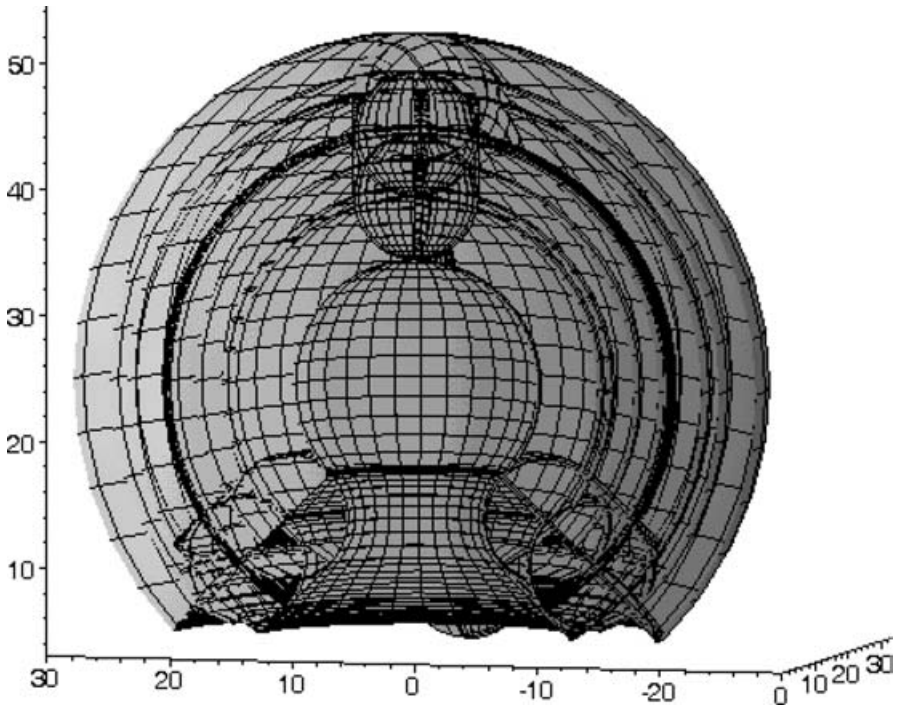


Fig. 7. A cross-section of the workspace of the 5-DOF RRPRR manipulator.

Applying the criteria in section 2 yields all singularity sets shown in the Appendix. Substituting all of the singular surfaces into Eq. (38) a cross-section of the workspace of a 5-DOF RRPRR manipulator is shown in Fig. 7.

## III. CONCLUSIONS

A general formulation for determining boundary surface patches in closed form to 5DOF manipulators with non-unilateral constraints has been presented. The workspace constraint function was formulated in terms of generalized coordinates including inequality constraints imposed on each joint's time function. It was shown that Jacobian rank-deficiency conditions usually applied in robotics analysis to determine degenerate conditions, are employed here to generate constant singular sets and to identify coupled singular behavior.

## References

1. I. Vinagradov, "Details of Kinematics of Manipulators with the Method of Volumes", (in Russian) *Mexanika Mashin*, **27–28**, 5–16 (1971).
2. B. Roth, "Performance Evaluation of Manipulators from a Kinematic Viewpoint", *NBS Special Publications* **459**, 39–61 (1975).
3. A. Kumar and K. J. Waldron, "The Workspace of a Mechanical Manipulator", *ASME J. Mech. Design* **103**, 665–672 (1981).
4. Y. C. Tsai and A. H. Soni, "Accessible Region and Synthesis of Robot Arm", *ASME J. of Mech. Design* **103**, 803–811 (1981).
5. K. G. Gupta and B. Roth, "Design Considerations for Manipulator Workspace", *ASME Journal of Mechanical Design* **104**(4), 704–711 (1982).
6. K. C. Gupta, "On the Nature of Robot Workspace", *Int. J. Rob. Res.* **5**(2), 112–121 (1986).
7. K. Sugimoto and J. Duffy, "Determination of Extreme Distances of a Robot Hand. Part 2: Robot Arms with Special Geometry", *ASME J. of Mechanical Design* **104**, 704–712 (1982).
8. J. K. Davidson and K. H. Hunt, "Rigid Body Location and Robot Workspace: Some Alternative Manipulator Forms", *ASME J. of Mechanisms, Transmissions, and Automation in Design* **109**(2), 224–232 (1987).
9. D. C. H. Yang and T. W. Lee, "On the Workspace of Mechanical Manipulators", *J. of Mechanisms, Transmission and Automation Design* **105**, 62–69 (1983).
10. S. K. Agrawal, "Workspace Boundaries of In-parallel Manipulator Systems", *Int. J. of Robotics and Automation* **7**(2), 94–99 (1990).
11. C. Gosselin and J. Angeles, "Singularity Analysis of Closed Loop Kinematic Chains", *IEEE Trans. on Robotics and Automation* **6**(3), 281–290 (1990).
12. D. M. Emiris, "Workspace Analysis of Realistic Elbow and Dual-elbow Robot", *Mechanisms and Machine Theory* **28**(3), 375–396 (1993).
13. G. R. Pennock and D. J. Kassner, "The Workspace of a General Planar Three-Degree-of-Freedom Platform-Type Manipulator", *Journal of Mechanical Design* **115**, 269–276 (1993).
14. M. Ceccarelli, "A Synthesis Algorithm for Three-Revolute Manipulators by Using an Algebraic Formulation of Workspace Boundary", *ASME J. of Mechanical Design* **117**(2A), 298–302 (1995).
15. S. J. Zhang, D. J. Sanger and D. Howard, "Workspaces of a Walking Machine and their Graphical Representation. Part I: Kinematic Workspaces", *Robotica* **14**, Part 1, 71–79 (1996).
16. E. J. Haug, C. M. Luh, F. A. Adkins and J. Y. Wang, "Numerical Algorithms for Mapping Boundaries of Manipulator Workspaces", *ASME J. Mech. Design* **118**, 228–234 (1996).
17. E. J. Haug, J. Y. Wang and J. K. Wu, "Dextrous Workspaces of Manipulators: I. Analytical Criteria", *Mech. Struct. and Mach.* **20**(3), 321–361 (1992).
18. J. Y. Wang and J. K. Wu, "Dexterous Workspaces of Manipulators, Part 2: Computational Methods", *Mechanics of Structures and Machines* **21**(4), 471–506 (1993).
19. C. C. Qiu, C. M. Luh and E. J. Haug, "Dexterous Workspaces of Manipulators, Part III: Calculation of Continuation Curves

https://doi.org/10.1017/S0263574704001262 Published online by Cambridge University Press

at Bifurcation Points", *Mechanics of Structures and Machines* **23**(1), 115–130 (1995).
20. M. Ceccarelli and A. Vinciguerra, "On the Workspace of General 4R Manipulators", *Int. J. Robotics Research* **14**(2), 152–160 (1995).
21. J. Spanos and D. Kohli, "Workspace Analysis of Regional Structure of Manipulators", *ASME J. of Mech. Trans. and Aut. in Design* **107**, 219–225 (1985).
22. H. Delmas, Workspace Analysis of Redundant Manipulators: Singularities and Parcourability, University of Bologna, *PhD thesis* (University of Bologna, 1996).
23. F. Bulca, J. Angeles and P. J. Zsombor-Murray, "On the Workspace Determination of Spherical Serial and Platform Mechanisms", *Mechanism & Machine Theory* **34**(3), 497–512 (1999).
24. J. Rastegar and P. Deravi, "Methods to Determine Workspace, its Subspaces with Different Numbers of Configurations and All the Possible Configurations of a Manipulator", *Mechanism and Machine Theory* **22**(4), 343–350 (1987).
25. G. S. Chirikjian and I. Ebert–Uphoff, "Numerical Convolution on the Euclidean Group with Applications to Workspace Generation", *IEEE Trans. Robot. Automat.* **14**, 123–136 (1998).
26. Y. Wang and G. S. Chirikjian, "Workspace Generation of Hyper-Redundant Manipulators as a Diffusion Process on *SE (N)*", *IEEE Transaction on Robotics and Automation* **20**(3), 399–408 (2004).
27. K. Abdel-Malek and H. J. Yeh, "Analytical Boundary of the Workspace for General 3-DOF mechanisms", *Int. J. Robotics Research* **16**(2), 1–12 (1997).
28. K. Abdel-Malek, H. J. Yeh and N. Khairallah, "Workspace, Void, and Volume Determination of the General 5DOF Manipulator", *Mechanics of Structures and Machines* **27**(1), 91–117 (1999).
29. J. Denavit and R. S. Hartenberg, "A Kinematic Notation for Lower-pair Mechanisms Based on Matrices", *Journal of Applied Mechanics* **22**, 215–221 (1955).
30. S. Fu, J. Gonzalez and S. Lee, Robotics: Control, *Sensing, Vision, And Intelligence* (McGraw-Hill, Inc., New York, 1987).

## APPENDIX

Singular sets:

$\mathbf{p}_1 = \{q_2(1.25), q_4(0), \text{and } q_5(1.57735)\}$ $\mathbf{p}_2 = \{q_2(0), q_4(0), \text{and } q_5(0.183503)\}$,
$\mathbf{p}_3 = \{q_2(0), q_4(0.275255), \text{and } q_5(1.57735)\}$ $\mathbf{p}_4 = \{q_2(0), q_4(1.5), \text{and } q_5(1.57735)\}$
$\mathbf{p}_5 = \{q_3(0), q_4(0), \text{and } q_5(0.183503)\}$ $\mathbf{p}_6 = \{q_2(1.25), q_3(0), \text{and } q_4(0)\}$,
$\mathbf{p}_7 = \{q_3(3.22474), q_4(0), \text{and } q_5(0)\}$ $\mathbf{p}_8 = \{q_2(1.25), q_3(3.22474), \text{and } q_4(0)\}$ ,
$\mathbf{p}_9 = \{q_2(0), q_3(0), \text{and } q_4(0.275255)\}$ $\mathbf{p}_{10} = \{q_2(0), q_3(3.22474), \text{and } q_4(0.275255)\}$
$\mathbf{p}_{11} = \{q_3(0) \text{ and } q_5(1.57735)\}$, $\mathbf{p}_{12} = \{q_3(3.22474) \text{ and } q_5(1.57735)\}$
$\mathbf{p}_{13} = \{q_3(2), q_4(1.5), q_5(1)\}$

$\mathbf{p}_{14} \ldots \mathbf{p}_{17}$ Four combinations $t_3 = 8$, $t_1 = \begin{Bmatrix} 0 \\ 2 \end{Bmatrix}$, $t_2 = \begin{Bmatrix} 0 \\ 2.5 \end{Bmatrix}$

$\mathbf{p}_{18} \ldots \mathbf{p}_{21}$ Four combinations $t_3 = 8$, $t_1 = \begin{Bmatrix} 0 \\ 2 \end{Bmatrix}$, $t_4 = \begin{Bmatrix} 0 \\ 2.36602 \end{Bmatrix}$

$\mathbf{p}_{22} \ldots \mathbf{p}_{25}$ Four combinations $t_3 = 8$, $t_1 = \begin{Bmatrix} 0 \\ 2 \end{Bmatrix}$, $t_5 = \begin{Bmatrix} 0 \\ 1.57735 \end{Bmatrix}$

$\mathbf{p}_{26} \ldots \mathbf{p}_{29}$ Four combinations $t_3 = 8$, $t_2 = \begin{Bmatrix} 0 \\ 2.5 \end{Bmatrix}$, $t_4 = \begin{Bmatrix} 0 \\ 2.36602 \end{Bmatrix}$

$\mathbf{p}_{30} \ldots \mathbf{p}_{33}$ Four combinations $t_3 = 8$, $t_1 = \begin{Bmatrix} 0 \\ 2.5 \end{Bmatrix}$, $t_5 = \begin{Bmatrix} 0 \\ 1.57735 \end{Bmatrix}$

$\mathbf{p}_{34} \ldots \mathbf{p}_{37}$ Four combinations $t_3 = 8$, $t_4 = \begin{Bmatrix} 0 \\ 2.36602 \end{Bmatrix}$, $t_5 = \begin{Bmatrix} 0 \\ 1.57735 \end{Bmatrix}$

$\mathbf{p}_{37} \ldots \mathbf{p}_{41}$ Four combinations $t_4 = 1.5$, $t_1 = \begin{Bmatrix} 0 \\ 2 \end{Bmatrix}$, $t_2 = \begin{Bmatrix} 0 \\ 2.5 \end{Bmatrix}$

$\mathbf{p}_{42} \ldots \mathbf{p}_{45}$ Four combinations $t_4 = 1.5$, $t_1 = \begin{Bmatrix} 0 \\ 2 \end{Bmatrix}$, $t_3 = \begin{Bmatrix} 0 \\ 3.22474 \end{Bmatrix}$

$\mathbf{p}_{46} \ldots \mathbf{p}_{49}$ Four combinations $t_4 = 1.5$, $t_1 = \begin{Bmatrix} 0 \\ 2 \end{Bmatrix}$, $t_5 = \begin{Bmatrix} 0 \\ 1.57735 \end{Bmatrix}$

$\mathbf{p}_{50} \ldots \mathbf{p}_{53}$ Four combinations $t_4 = 1.5$, $t_2 = \begin{Bmatrix} 0 \\ 2.5 \end{Bmatrix}$, $t_3 = \begin{Bmatrix} 0 \\ 3.22474 \end{Bmatrix}$

$\mathbf{p}_{54} \ldots \mathbf{p}_{57}$ Four combinations $t_4 = 1.5$, $t_2 = \begin{Bmatrix} 0 \\ 2.5 \end{Bmatrix}$, $t_5 = \begin{Bmatrix} 0 \\ 1.57735 \end{Bmatrix}$

$\mathbf{p}_{58} \ldots \mathbf{p}_{61}$ Four combinations $t_4 = 1.5$, $t_3 = \begin{Bmatrix} 0 \\ 3.22474 \end{Bmatrix}$, $t_5 = \begin{Bmatrix} 0 \\ 1.57735 \end{Bmatrix}$

https://doi.org/10.1017/S0263574704001262 Published online by Cambridge University Press

$\mathbf{p}_{62} \ldots \mathbf{p}_{65}$ Four combinations $t_5 = 1.0$, $t_1 = \begin{Bmatrix} 0 \\ 2 \end{Bmatrix}$, $t_2 = \begin{Bmatrix} 0 \\ 2.5 \end{Bmatrix}$

$\mathbf{p}_{66} \ldots \mathbf{p}_{69}$ Four combinations $t_5 = 1.0$, $t_1 = \begin{Bmatrix} 0 \\ 2 \end{Bmatrix}$, $t_3 = \begin{Bmatrix} 0 \\ 3.22474 \end{Bmatrix}$

$\mathbf{p}_{70} \ldots \mathbf{p}_{74}$ Four combinations $t_5 = 1.0$, $t_1 = \begin{Bmatrix} 0 \\ 2 \end{Bmatrix}$, $t_4 = \begin{Bmatrix} 0 \\ 2.36602 \end{Bmatrix}$

$\mathbf{p}_{75} \ldots \mathbf{p}_{78}$ Four combinations $t_5 = 1.0$, $t_2 = \begin{Bmatrix} 0 \\ 2.5 \end{Bmatrix}$, $t_3 = \begin{Bmatrix} 0 \\ 3.22474 \end{Bmatrix}$

$\mathbf{p}_{79} \ldots \mathbf{p}_{82}$ Four combinations $t_5 = 1.0$, $t_2 = \begin{Bmatrix} 0 \\ 2.5 \end{Bmatrix}$, $t_4 = \begin{Bmatrix} 0 \\ 2.36602 \end{Bmatrix}$

$\mathbf{p}_{83} \ldots \mathbf{p}_{86}$ Four combinations $t_5 = 1.0$, $t_3 = \begin{Bmatrix} 0 \\ 3.22474 \end{Bmatrix}$, $t_4 = \begin{Bmatrix} 0 \\ 2.36602 \end{Bmatrix}$

$\mathbf{p}_{87} \ldots \mathbf{p}_{88}$ Two combinations $t_3 = 2.0$, $t_5 = 0$, $t_4 = \begin{Bmatrix} 0 \\ 2.36602 \end{Bmatrix}$

$\mathbf{p}_{89} \ldots \mathbf{p}_{90}$ Two combinations $t_3 = 2.0$, $t_5 = 0$, $t_2 = \begin{Bmatrix} 0 \\ 2.5 \end{Bmatrix}$

$\mathbf{p}_{91} \ldots \mathbf{p}_{92}$ Two combinations $t_3 = 2.0$, $t_5 = 0$, $t_1 = \begin{Bmatrix} 0 \\ 2 \end{Bmatrix}$

$\mathbf{p}_{93} \ldots \mathbf{p}_{94}$ Two combinations $t_2 = \frac{\pi}{2}$, $t_5 = \pi$, $t_1 = \begin{Bmatrix} 0 \\ 2 \end{Bmatrix}$

$\mathbf{p}_{95} \ldots \mathbf{p}_{96}$ Two combinations $t_2 = \frac{\pi}{2}$, $t_5 = \pi$, $t_3 = \begin{Bmatrix} 0 \\ 3.22474 \end{Bmatrix}$

$\mathbf{p}_{97} \ldots \mathbf{p}_{98}$ Two combinations $t_2 = \frac{\pi}{2}$, $t_5 = \pi$, $t_4 = \begin{Bmatrix} 0 \\ 2.36602 \end{Bmatrix}$

https://doi.org/10.1017/S0263574704001262 Published online by Cambridge University Press